

# Biomaterials for CO<sub>2</sub> Harvesting: From Regulatory Functions to Wet Scrubbing Applications

Khaleel I. Assaf,<sup>\*,†</sup> Abdussalam K. Qaroush,<sup>\*,‡</sup> Farah M. Mustafa,<sup>§</sup> Fatima Alsoubani,<sup>§</sup> Thomas M. Pehl,<sup>||</sup> Carsten Troll,<sup>||</sup> Bernhard Rieger,<sup>||</sup> and Ala'a F. Eftaiha<sup>\*,§</sup>

<sup>†</sup>Department of Chemistry, Faculty of Science, Al-Balqa Applied University, PO Box 19117, Al-Salt, Jordan

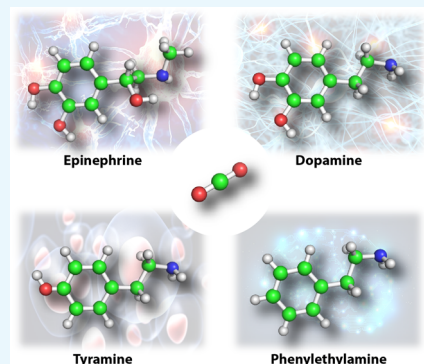
<sup>‡</sup>Department of Chemistry, Faculty of Science, The University of Jordan, Amman 11942, Jordan

<sup>§</sup>Department of Chemistry, The Hashemite University, PO Box 150459, Zarqa 13115, Jordan

<sup>||</sup>WACKER-Lehrstuhl für Makromolekulare Chemie, Technische Universität München, Lichtenbergstraße 4, 85747 Garching bei München, Germany

## Supporting Information

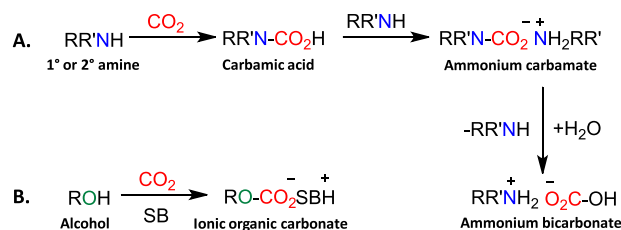
**ABSTRACT:** A new series of 2-aminoethyl-benzene-based biomaterials, namely, dopamine (DOP), tyramine (TYR), phenylethylamine (PEA), and epinephrine (EPN), dissolved in dimethylsulfoxide (DMSO) have been investigated for CO<sub>2</sub> capture upon activating their hydrochloride salts with a NaOH pellet. Spectroscopic measurements, including ex situ ATR-FTIR, 1D and 2D NMR experiments have been applied to verify the formation of the sodium carbamate adducts (RR'N-CO<sub>2</sub><sup>-</sup> Na<sup>+</sup>). The emergence of new peaks in the IR spectra ranging between 1702 and 1735 cm<sup>-1</sup> together with the chemical shift within 157–158 ppm in the <sup>13</sup>C NMR, as well as with cross-peaks obtained by <sup>1</sup>H-<sup>15</sup>N HSQC measurements at ca. 84 and 6.6 ppm verified the formation of RR'N-CO<sub>2</sub><sup>-</sup> Na<sup>+</sup> products upon the chemical fixation of CO<sub>2</sub>. The CO<sub>2</sub> sorption capacity of the examined biomaterials was evaluated volumetrically, with a maximum value of 8.18 mmol CO<sub>2</sub>·g<sup>-1</sup> sorbent (36.0 (w/w)%), including both chemisorption and physisorption, for 5 (w/v)% solutions measured at 5 bar CO<sub>2</sub> and 25 °C, for TYR and PEA. DFT calculations indicated that the intramolecular hydrogen bonding within the structural motif of EPN-N-CO<sub>2</sub><sup>-</sup> Na<sup>+</sup> adduct provides an exceptional stability compared to monoethanolamine and other structurally related model compounds.



## 1. INTRODUCTION

Fossil fuels consumption associated with emitting huge amounts of CO<sub>2</sub> is directly connected to the global warming phenomenon.<sup>1</sup> The negative consequences of climate change directed the efforts of politicians and scientists to legislate restrict policies and find new approaches to mitigate further CO<sub>2</sub> accumulation in the atmosphere to avoid the catastrophic two-degree scenario above the preindustrial revolution era.<sup>2,3</sup> Currently, there are four main approaches to alleviate this problem, which are carbon capture and sequestration (CCS), direct air capture (DAC), carbon capture and recycling (CCR), and capture and utilization (CCU). The ultimate goal of CCS and DAC is to store and, for the latter, most probably exploit CO<sub>2</sub> as a renewable feedstock in the fine chemical industry, which might be dealt with on a later stage as CCU.<sup>4,5</sup> The sorption of CO<sub>2</sub> takes place via either physisorption or chemisorption. Either processes might require the presence of a nucleophilic atom (e.g., N or O), which results in the formation of carbamic acid (RR'N-CO<sub>2</sub>H)/carbamate (RR'N-CO<sub>2</sub><sup>-</sup> X<sup>+</sup>; X: sacrificial base, or metal) or carbonate (ionic organic (RO-CO<sub>2</sub><sup>-</sup> X<sup>+</sup>)/inorganic X<sub>n</sub>CO<sub>3</sub>) adducts (Scheme 1).<sup>6</sup> Primary and secondary amines are known to directly attack CO<sub>2</sub> to form the organic CO<sub>2</sub>

**Scheme 1. CO<sub>2</sub> Reaction Pathways with: (A) Interaction of CO<sub>2</sub> with Amines at Dry and Wet Conditions, (B) Alcohols in the Presence of a Superbase (SB), Following 1:2 (Carbamate) and 1:1 (Carbamic Acid or Organic Carbonate) Reaction Mechanism<sup>a</sup>**



<sup>a</sup>The presence of water and ammonium carbamate (in (A)) results in the formation of inorganic bicarbonate.

sequestered adduct(s), while tertiary amines lack transferable protons and tend to form inorganic bicarbonates exclusively in aqueous media.<sup>7</sup>

**Received:** April 5, 2019

**Accepted:** June 17, 2019

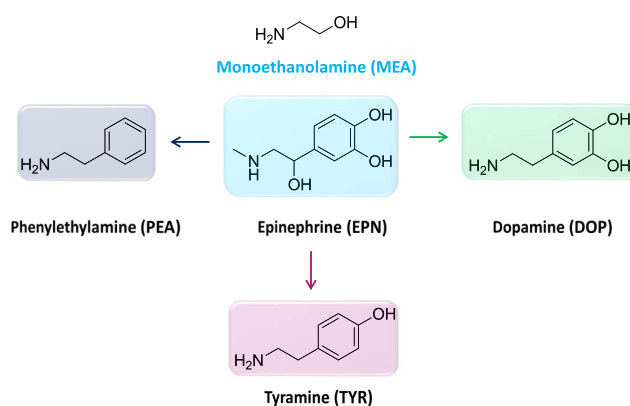
**Published:** July 2, 2019

Aqueous amine solutions are considered the most economical technology for postcombustion CO<sub>2</sub> capture. In this respect, 30 wt % aqueous monoethanolamine (MEA) solution (with a sorption capacity 7 wt %) is extensively studied since its patented by Bottoms in 1930.<sup>9</sup> The intrinsic drawbacks of aqueous amine solutions such as high regeneration temperatures, thermal degradation, and evaporation losses moved the attention of scientists into sterically hindered amines, which are primary or secondary amine-based compounds where the amino groups are attached to a tertiary carbon or a secondary/tertiary carbon, respectively. They tend to form relatively unstable carbamates with fast reaction kinetics compared to conventional amine wet scrubbing agents.<sup>10,11</sup> As a breakthrough, the use of task-specific ionic liquids (TSILs), namely, (1-*n*-propylamine-3-butylimidazolium tetrafluoroborate), showed 7.4 wt % gain due to CO<sub>2</sub> capture.<sup>12</sup> Other TSILs, including conventional and reversible ILs, are used for CO<sub>2</sub> capturing technology, as reviewed by Park and co-workers.<sup>13</sup> Moreover, CO<sub>2</sub>-binding organic liquids (CO<sub>2</sub>-BOLs), which are composed of alcohols and organic superbases (SBs), such as amidines or guanidines containing SB, that chemically bind CO<sub>2</sub> as ionic organic carbonate, with a CO<sub>2</sub> sorption capacity of 19 wt %, <sup>8,14,15</sup> and the use of polar aprotic solvents, represents another alternative method.<sup>16–18</sup> In this context, green chemistry offers an opportunity for chemists and engineers to design benign routes by preventing waste and eliminating the need for energy-intensive processes to ultimately achieve sustainable development.<sup>19</sup> Of particular importance, in our study, is to follow and enhance green chemistry principles that highlights the implementation of renewable feedstocks for CO<sub>2</sub> capturing (for a broad overview about green chemistry, the readers are directed toward review articles by Paul Anastas and co-workers<sup>20–22</sup>).

Our research group and others have utilized green, as well as oxygen- and nitrogen-rich synthetic and/or biofeedstock sorbents such as oligourea,<sup>23</sup> cellulose,<sup>24–26</sup> chitin/chitosan,<sup>27–31</sup> and cyclodextrin<sup>32,33</sup> as solid and wet sorbents for CO<sub>2</sub> capturing via supramolecular chemisorption or activation by superbases through the formation of RO-CO<sub>2</sub><sup>-</sup> Y<sup>+</sup> (Y<sup>+</sup>: organic or inorganic counter cation). Moreover, Stoddart and co-workers reported on the synthesis and characterization of a series of metal organic frameworks (MOFs) composed of  $\gamma$ -cyclodextrin that chemisorbed CO<sub>2</sub> reversibly<sup>34–37</sup> (see ref 38 for more examples). Other nitrogen-rich biomaterials such as amino acids were found to be effective for CO<sub>2</sub> capturing through the formation of ammonium carbamate or carbamic acid adducts. Bhattacharyya and Shah reported on the use of a series of low-viscosity, choline (Cho)-based amino acid ILs to capture CO<sub>2</sub> with a reasonable sorption capacity of ca. 19 wt %.<sup>39</sup> In addition, Zou's group<sup>40</sup> and others<sup>41</sup> explored the mechanism of CO<sub>2</sub> binding by neat Cho-proline IL and its solution in nonaqueous solvents (including poly(ethylene glycol) and dimethylsulfoxide, DMSO), with a sorption capacity of 0.6:1 M ratio of CO<sub>2</sub>-IL at approximately 1 bar pressure.<sup>40</sup> The mechanism of CO<sub>2</sub> sorption by the aqueous solutions of Cho-ILs composed of alanine, proline, and glycine indicated the formation of carbamate adduct at low concentration and inorganic carbonate if the concentration exceeded 5 wt %.<sup>42</sup> Such materials were further exploited as catalysts for cyclic carbonate synthesis.<sup>43</sup>

Very recently, our group has reported on the chemisorption of CO<sub>2</sub> by biomaterials, viz., epinephrine,<sup>44</sup> (EPN, a catecholamine neurotransmitter, Scheme 2) when dissolved in DMSO

**Scheme 2. Chemical Structure of Epinephrine (EPN) with Its Model Compound MEA, and Other Biomaterial Counterparts<sup>a</sup>**



<sup>a</sup>Dopamine (DOP), tyramine (TYR), and phenylethylamine (PEA).

through the formation of alkali metal carbamate (RR'NCO<sub>2</sub><sup>-</sup>X<sup>+</sup>) upon activation of its acidic form with a metal hydroxide. According to National Institutes of Health, biomaterials are defined as any matter, surface, or construct that interacts with biological systems that can be derived from nature or synthesized in the laboratory using metallic components, polymers, ceramics, or composite materials. The aim of this work is to investigate selected biomaterials with common structural motifs of EPN-like compounds, viz., dopamine (DOP), tyramine (TYR), and phenylethylamine (PEA), as shown in Scheme 2. The impact of the amine category (primary or secondary), the catecholic or phenolic part, and the absence of the aliphatic hydroxyl group are all considered in exploring the overall mechanism of CO<sub>2</sub> capturing. The reaction of these biomaterials with CO<sub>2</sub> has been investigated using nuclear magnetic resonance (NMR) and ex situ attenuated total reflectance-Fourier transform infrared (ATR-FTIR) spectroscopy techniques. Moreover, volumetric CO<sub>2</sub> uptake was measured using an in situ ATR-FTIR autoclave equipped with a digital manometer. Furthermore, density functional theory (DFT) calculations were employed to explore the mechanism of carbamation reactions.

## 2. RESULTS AND DISCUSSION

Under air conditions, the color change associated with EPN-HCl upon activation with a metal hydroxide<sup>44</sup> is an indicator of oxidation as a result of hydroquinone/quinone conversion,<sup>45</sup> which motivates exploring the stability of related biomaterial architectures. The photographs of EPN-HCl, DOP-HCl, TYR-HCl, and PEA-HCl dissolved in DMSO before and after activation with a NaOH pellet are shown in Figure 1. Although it is poorly soluble in DMSO ( $\leq 1$  mg/mL),<sup>46</sup> L-3,4-dihydroxyphenylalanine (L-DOPA, the precursor of EPN and DOP, another catecholamine neurotransmitter) was used as a control sample. The obtained color change after sonication in the presence of the base indicated that EPN and DOP were readily oxidized, followed by L-DOPA and TYR, while no change was observed in the case of PEA. After 24 h, the TYR solution resisted the oxidation to some extent in comparison to L-DOPA, while PEA solution indicated excellent stability. Similar to PEA, ephedrine (with no phenolic or catecholic functionalities) is more structurally related to EPN; however, it

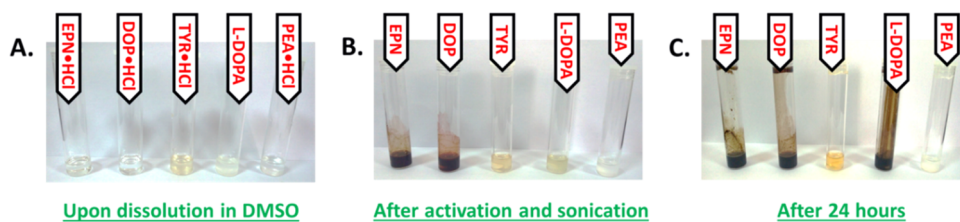


**Figure 1.** Photographs of EPN·HCl, DOP·HCl, TYR·HCl, L-DOPA, and PEA·HCl solutions in DMSO: (A) readily after preparation, (B) and (C) upon activation with NaOH after 10 min and 24 h, respectively (Photograph courtesy of ‘Farah Mustafa’, Copyright 2019).

is categorized as prescription-controlled material, which restricted its commercial availability for further testing.

DOP is structurally similar to EPN, except the presence of a primary rather than secondary amine group and the absence of the aliphatic hydroxyl group as shown in Scheme 2. The  $^{13}\text{C}$  NMR spectrum of DOP·HCl dissolved in DMSO- $d_6$  shows eight peaks related to its backbone and an additional one at 124.2 ppm upon bubbling  $\text{CO}_2$  corresponding to the physically sorbed  $\text{CO}_2$  (Figure S1, Supporting Information, SI). After activation using NaOH, the  $^{13}\text{C}$  NMR spectrum of DOP confirmed the chemisorption of  $\text{CO}_2$  by emerging new chemical shifts centered at 157 and 158 ppm (Figure A2). This indicated the reaction of DOP with  $\text{CO}_2$  in the presence of NaOH along with the formation of both DOP-N- $\text{CO}_2^- \text{Na}^+$  and inorganic bicarbonate.<sup>44</sup>

Moreover, TYR, a biogenic amine formed by the enzymatic decarboxylation of tyrosine,<sup>47</sup> dissolved in DMSO- $d_6$ , showed a similar response compared to DOP·HCl by the emergence of two new peaks in the  $^{13}\text{C}$  NMR measurement within the region 157–158 ppm (Figure B2), which also indicated the same mechanism (vide supra) of interaction with  $\text{CO}_2$  as in the case of DOP.

The potential carbamation reactions of DOP·HCl and its neutral basic form dissolved in DMSO were further explored using ex situ ATR-FTIR spectroscopy before (green trace) and after (blue trace) bubbling  $\text{CO}_2$ . As presented in Figure 2 and

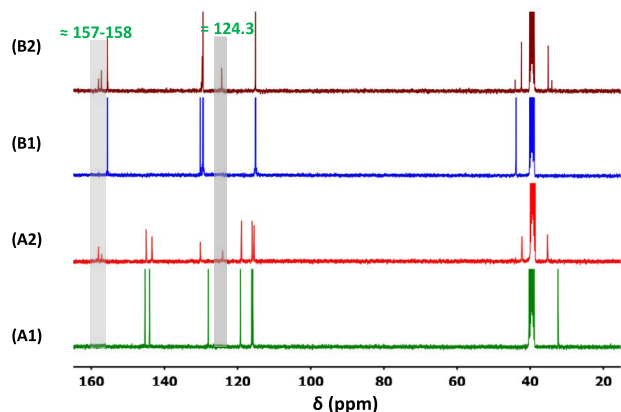


**Figure 2.**  $^{13}\text{C}$  NMR spectra of (A) DOP·HCl and (B) TYR·HCl: (1) upon dissolution in DMSO- $d_6$  and (2) after the addition of NaOH in DMSO- $d_6$  solution under  $\text{CO}_2$  atmosphere

3A, the peak at  $2337\text{ cm}^{-1}$  represented the asymmetric stretching of the physisorbed  $\text{CO}_2$ , while the peak at  $1718\text{ cm}^{-1}$  denoted the formation of DOP-N- $\text{CO}_2^- \text{Na}^+$ , which verified the results obtained by  $^{13}\text{C}$  NMR spectroscopy and in a good agreement with the results recorded previously for EPN.<sup>44</sup> Moreover, the ATR-FTIR spectra of TYR fortified the

chemisorption of  $\text{CO}_2$  through the emergence of a new peak at  $1701\text{ cm}^{-1}$  (Figure 3B).

Supported by the visual color change of the activated biomaterials (vide supra), the anticipated stability of PEA (a naturally occurring amine that resembles an amphetamine from both pharmacological and structural aspects)<sup>48</sup> due to the absence of catecholic functionality, triggered further investigation toward  $\text{CO}_2$  capturing. Upon dissolving in DMSO and activation with an NaOH pellet,  $^{13}\text{C}$  NMR and ATR-FTIR measurements confirmed the formation of a solely captured species (PEA-N- $\text{CO}_2^- \text{Na}^+$ ) due to the emergence of new peaks around 157 ppm and  $1702\text{ cm}^{-1}$ , respectively (Figure 4). The difference in chemical shift between the starting materials and the sequestered adducts of DOP, TYR, and PEA is shown in Table S1, SI. The most drastic difference was observed between the neighboring and the second neighboring carbons to the nitrogen, which confirmed the formation of the suggested carbamate adduct.

To ensure that the carbamation reaction occurred at the nitrogen atom of the various 2-aminoethyl-benzene scaffolds,  $^1\text{H}$ - $^{15}\text{N}$  heteronuclear single quantum coherence spectroscopy (HSQC) measurements were performed. After activation and bubbling with  $\text{CO}_2$ , the 2D spectra of the three compounds indicated a downfield  $^{15}\text{N}$  chemical shift (observed at ca. 84 ppm, Figure 5) in comparison to the primary aliphatic ammonium ions that ranged between 20 and 60 ppm.<sup>49</sup> This is consistent with our previous measurements using EPN.<sup>44</sup>

**2.1. Volumetric Uptake Measurements.** The sorption capacity of 5 (w/v)% solutions of the examined substrates dissolved in DMSO was measured using an in situ ATR-FTIR autoclave coupled with a digital manometer. The amount of the sorbed  $\text{CO}_2$  was calculated volumetrically upon substituting the pressure drop after correction against DMSO in the equation of state of ideal gas ( $PV = nRT$ ), and the results are presented in Table 1. The results indicated that EPN sorbed  $1.64\text{ mmol CO}_2\cdot\text{g}^{-1}$  sorbent, while DOP (the other structurally similar substrate) exhibited only half the sorption capacity, with  $0.82\text{ mmol CO}_2\cdot\text{g}^{-1}$  sorbent. This behavior was attributed to the extra ion–dipole interaction between the metal carbamate and the aliphatic hydroxyl group of EPN, which is absent in the case of DOP. This offers a distinct stability of the sequestered adduct and thus better performance characteristics of EPN over the latter as inferred from reaction free-energy values that were obtained from the DFT calculations (vide infra). In a similar context, TYR and PEA showed larger sorption capacity values with  $2.46\text{ mmol CO}_2\cdot\text{g}^{-1}$  sorbent. A partial in situ ATR-FTIR spectrum of PEA solution is shown in Figure 4C. An in-depth insight into the chemical structure of the 2-aminoethyl-benzene moieties shows that both PEA and TYR have more nonpolar character (benzene and phenol, respectively) compared to the other catecholic moieties and tend to be more  $\text{CO}_2$ -philic, which might explain the better



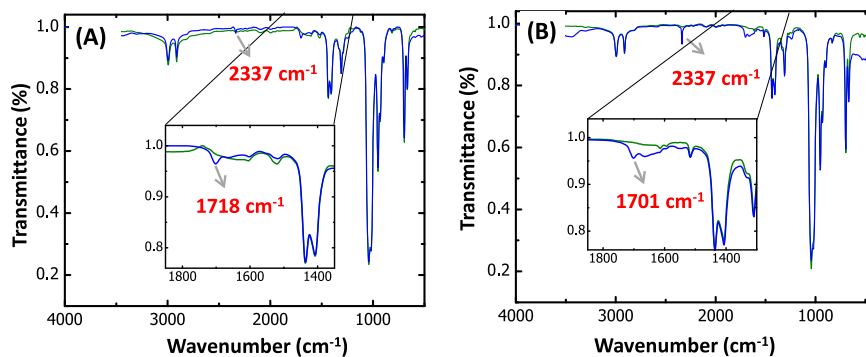


**Figure 3.** ATR-FTIR spectra of: (A) DOP-HCl and (B) TYR-HCl solutions before (green) and after (blue) activation with NaOH and bubbling with CO<sub>2</sub>, respectively.

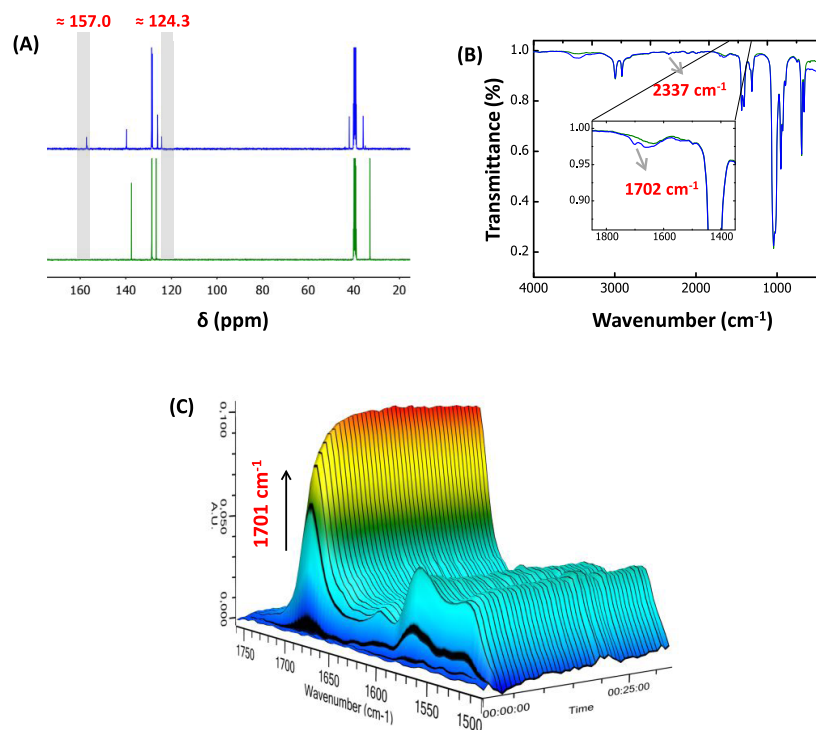


**Figure 4.** (A) <sup>13</sup>C NMR spectra of PEA-HCl/DMSO-*d*<sub>6</sub> (green trace), under CO<sub>2</sub> atmosphere upon activation with NaOH (blue trace). (B) ATR-FTIR spectrum before (green trace) and after activation with NaOH and bubbling CO<sub>2</sub> (blue trace). (C) Partial in situ ATR-FTIR spectrum for the 5% (w/v) PEA/DMSO activated with NaOH as a function of time carried out at 25 °C and 5.0 bar.

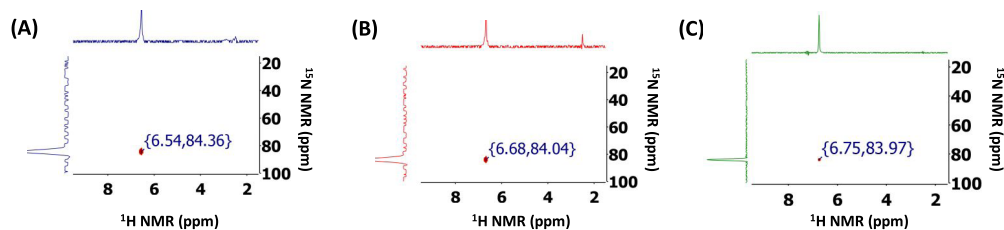


**Figure 5.** <sup>1</sup>H-<sup>15</sup>N HSQC spectra of: (A) DOP, (B) TYR, and (C) PEA in DMSO-*d*<sub>6</sub> with CO<sub>2</sub> bubbling after activation with NaOH.

performance. The sorption capacity of the latter two compounds was so close with that obtained for MEA under the same experimental conditions, which might be an excellent indicator for a similar mechanism of the examined biomaterial compounds with CO<sub>2</sub> action and the benchmark sorbent.

The absence of universal protocols to evaluate the CO<sub>2</sub> capture in terms of the measurement techniques and the sorption conditions make it hard to hold a fair comparison

between the sorption capacities of different sorbents. However, such comparison provides a useful indicator for assessing the performance characteristics of the examined systems. In comparison to other nitrogen-rich, biorenewable CO<sub>2</sub>-philes reported previously such as chitin and chitosan dissolved in different solvents such as ILs,<sup>27</sup> DMSO,<sup>30,31</sup> or even neat lysine-based IL,<sup>39</sup> our measurements showed comparable sorption capacity values. However, we cannot overemphasize

**Table 1. Volumetric Uptake Measurements<sup>a</sup> of 5 (w/v)% Solutions of Different 2-Aminoethyl-benzene-Based Moieties Dissolved in DMSO and Activated by a NaOH Pellet Using in Situ ATR-FTIR Autoclave Pressurized with 5 Bar CO<sub>2</sub> at 25 °C<sup>b</sup>**

	EPN	DOP	TYR	PEA	MEA
pressure drop (bar)	0.4	0.2	0.6	0.6	0.8
sorption capacity mmol CO <sub>2</sub> ·g <sup>-1</sup> sorbent	1.64	0.82	2.46	2.46	3.27
scrubbing agent	sorption capacity (mmol CO <sub>2</sub> ·g <sup>-1</sup> sorbent)	mechanism of action/sequestered adduct			conditions
chitin/[Bmim]Cl, <sup>27c</sup>	2.17 <sup>d</sup>	physisorption			10 wt %, 30 °C, and 1 bar
chitosan/[Bmim]Cl, <sup>27c</sup>	4.64 <sup>d</sup>	physisorption and chemisorption/carbamate adduct			10 wt %, 30 °C, and 1 bar
chitin acetate/DMSO <sup>30</sup>	3.63 <sup>e</sup>	supramolecular chemisorption/organic carbonate formation			10 (w/v)%, 25 °C, and 4 bar
oligo-chitosan/DMSO <sup>31</sup>	1.64 <sup>e</sup>	supramolecular chemisorption/organic carbonate-carbamate adduct			10 (w/v)%, 25 °C, and 4.2 bar
choline-based lysine IL <sup>39</sup>	4.32 <sup>d</sup>	chemisorption/carbamic acid, carbamate adduct			ca. 1 g, 20 °C, and 1 bar

<sup>a</sup>The amount of the sorbed CO<sub>2</sub> was calculated from the pressure drop obtained from the manometer, applying the equation of state of ideal gas ( $PV = nRT$ ). The measurements were corrected against the physisorbed CO<sub>2</sub> using DMSO (1.4 bar) as a control sample. <sup>b</sup>In addition, a comparison with other nitrogen-rich bio-renewables reported in the literature is presented. <sup>c</sup>1-Butyl-3-methyl-imidazolium chloride. <sup>d</sup>Gravimetric uptake measurement. <sup>e</sup>Volumetric uptake measurement.

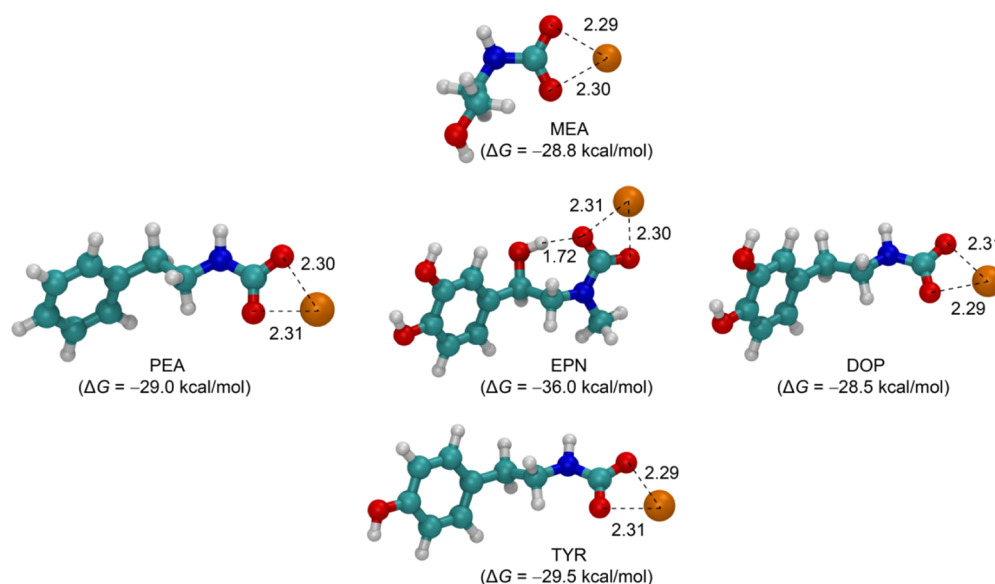


**Figure 6.** DFT-optimized structures of EPN, MEA, DOP, TYR, PEA, and the associated reaction free energy ( $\Delta G$  in kcal/mol) for the chemical fixation of CO<sub>2</sub> in DMSO upon activation with NaOH.

on results due to the different mechanism of action, as shown in Table 1.

**2.2. Quantum Chemical Calculations.** The reaction of 2-aminoethyl-benzene-based biomaterials with CO<sub>2</sub> was also investigated using quantum chemical calculations, in addition to MEA as a reference compound. The geometry of the anticipated products was optimized in DMSO as an implicit solvent, applying the polarizable continuum model (PCM). Minima were characterized by the absence of imaginary frequencies. In principle, the substrates are capable of reacting with CO<sub>2</sub> and produce the correspondent carbamate adducts in after activation with NaOH. Although the hydroxyl groups are also potential reaction sites, previous DFT calculations with EPN showed that the amine groups are more reactive.<sup>44</sup> Figure 6 shows the optimized structure of the sequestered products, and the carbamate ( $-\text{NCOO}^-$ ) adduct is stabilized by ion–ion interaction with Na<sup>+</sup>, as indicated by the short interaction distances (Figure 6). In the case of EPN, the structure of the formed adduct is stabilized by an additional intramolecular hydrogen bond (ca. 1.72 Å) between one of the oxygens on the carbamate group and the adjacent hydroxyl group (Figure 6).

This further verified the volumetric uptake measurement of EPN.

The reaction free energies ( $\Delta G$ ) for all reactions were calculated for the formation of the metal carbamate; the calculated values are given in Figure 6. The calculated  $\Delta G$  values for the carbamation reactions were negative for all of the investigated compounds, indicating a favorable process. Moreover, the latter values indicated that the formation of the carbamate adduct is the most favorable in the case of EPN ( $\Delta G = 36$  kcal/mol) compared to the other amines, which was in accordance with the additional stabilization through the hydrogen bonding of the neighboring hydroxyl group with no significant differences recorded for the other substrates ( $\Delta G \sim 29$  kcal/mol). The reaction of 2-aminoethyl-benzene-based biomaterials followed the order  $\text{EPN} \gg \text{PEA} > \text{TRY} > \text{MEA} > \text{DOP}$ . It is also anticipated that the hydroxyl groups on the benzene ring do not have a substantial effect on the reaction.

### 3. CONCLUSIONS

In this work, we presented a basic understanding of using several 2-aminoethyl-benzene-based biomaterial moieties dis-

solved in DMSO for CO<sub>2</sub> capture. Both NMR and ATR-FTIR spectroscopic measurements supported the chemisorption of CO<sub>2</sub> through the formation of sodium carbamate adduct. The volumetric CO<sub>2</sub> uptake data indicated that the best sorption capacity was achieved by tyramine and phenylethylamine, while DFT calculations showed that epinephrine-sodium carbamate was the most stable adduct among the other investigated compounds even when compared to monoethanolamine. The extra stability was attributed to short-range intermolecular forces.

## 4. EXPERIMENTAL SECTION

**4.1. Chemicals.** All reagents were obtained from commercial suppliers and used without further purification. Epinephrine hydrochloride (EPN·HCl), dopamine hydrochloride (DOP·HCl), tyramine hydrochloride (TYR·HCl), dimethylsulfoxide (DMSO-*d*<sub>6</sub>, 99.5 atom % D), and monoethanolamine (MEA, 98%, *d* = 1.012 g·mL<sup>-1</sup>) were purchased from Sigma-Aldrich. 2-Phenylethylamine hydrochloride (PEA·HCl, 99%) and (DMSO, 99.8%) were purchased from Fluka and TEDIA, respectively. L-3,4-dihydroxyphenylalanine (L-DOPA, 98.5%) was purchased from S D Fine-Chem Ltd. The hydroxide bases NaOH and KOH (as pellets) were obtained from Gainland Chemical Co. and Net Tech Ltd., respectively. CO<sub>2</sub> (industrial grade) and N<sub>2</sub> (industrial grade) were purchased from Advanced Technical Gases Co. (Amman, Jordan).

**4.2. Instruments.** Solution <sup>1</sup>H, <sup>13</sup>C, and <sup>15</sup>N nuclear magnetic resonance (NMR) spectra were collected at room temperature using (AVANCE- III 400 MHz (<sup>1</sup>H: 400.13 MHz, <sup>13</sup>C: 100.61 MHz, <sup>15</sup>N: 40.560 MHz) FTNMR NanoBay spectrometer (Bruker, Switzerland). Ex situ ATR-FTIR spectra were recorded using a Bruker Vertex 70-FT-IR spectrometer at room temperature coupled with a Vertex Pt-ATR-FTIR accessory. In situ ATR-FTIR measurements were carried out using an MMR45 m RB04-50 (Mettler Toledo, Switzerland) with an MCT detector with a diamond-window probe connected via a pressure vessel.

**4.3. Experimental Procedures.** In a Schlenk flask, 40 mg (0.2 mmol) of DOP·HCl was dried under vacuum for 2 h, then dissolved in 1.0 mL of DMSO-*d*<sub>6</sub>, stirred and bubbled with CO<sub>2</sub> under Schlenk line for 30 min before and after activation using KOH (ca. 203 mg, 3.6 mmol) and NaOH (ca. 513 mg, 12.8 mmol) pellets. In the same manner, TYR·HCl (ca. 25 mg, 0.14 mmol) and PEA·HCl (ca. 32 mg, 0.2 mmol) were directly dissolved in 1.0 mL of DMSO-*d*<sub>6</sub>, activated with KOH (ca. 184 mg, 3.3 mmol) and NaOH (ca. 492 mg, 12.3 mmol) under CO<sub>2</sub> bubbling and stirring for 30 min. For the ex situ ATR-FTIR measurements, the same procedures were followed by using DMSO rather than the deuterated solvent. For comparison purposes, the spectroscopic results of the samples activated by KOH are shown in the Supporting Information.

For the volumetric CO<sub>2</sub> measurements, a 5% (w/v) solution of scrubbing agent (EPN, DOP·HCl, TYR, PEA, or MEA) and DMSO is prepared in an argon-filled glovebox. After addition of a NaOH pellet and sonication for 20–40 min, 10 mL of the solution is transferred to an autoclave. The solution is stirred at 500 rpm for 3 min, followed by pressurizing the autoclave with 5 bar CO<sub>2</sub>. The reaction is monitored for 30 min until reaching a constant pressure. For the color visualization experiment, 30 mg of each molecule was dissolved in 1.0 mL of DMSO using a 10.0 mL vial and sonicated for 10 min upon activation using NaOH pellet (281 mg, 7.0 mmol).

**4.4. DFT Calculations.** DFT calculations were performed using the M06-2X functional and the 6-311G\*\* basis set in Gaussian 09 package. The molecular structure of the compounds in ground state was optimized in DMSO as an implicit solvent, applying the polarizable continuum model (PCM), and found to be minima, as indicated by the absence of imaginary frequencies.

## ■ ASSOCIATED CONTENT

### Supporting Information

The Supporting Information is available free of charge on the ACS Publications website at DOI: 10.1021/acsomega.9b00978.

<sup>13</sup>C NMR spectra of DOP·HCl dissolved in DMSO-*d*<sub>6</sub> before and after bubbling CO<sub>2</sub>; <sup>13</sup>C NMR spectrum of DOP·HCl and TYR·HCl dissolved in DMSO-*d*<sub>6</sub>, and after activation with KOH under CO<sub>2</sub> atmosphere; ATR-FTIR spectra of DOP·HCl and TYR·HCl solutions before and after activation with KOH and bubbling with CO<sub>2</sub>; <sup>13</sup>C NMR and ATR-FTIR spectra of PEA·HCl/DMSO-*d*<sub>6</sub> under CO<sub>2</sub> atmosphere upon activation with KOH and bubbling CO<sub>2</sub>; <sup>13</sup>C NMR chemical shifts ( $\delta$ , ppm) of selected carbon atoms along the skeleton of DOP, TYR, and PEA; <sup>1</sup>H-<sup>15</sup>N HSQC spectra of DOP, TYR, and PEA in DMSO-*d*<sub>6</sub> with CO<sub>2</sub> bubbling after activation with KOH (PDF)

## ■ AUTHOR INFORMATION

### Corresponding Authors

\*E-mail: khaleel.assaf@bau.edu.jo (K.I.A.).

\*E-mail: a.qaroush@ju.edu.jo (A.K.Q.).

\*E-mail: alaa.eftaiha@hu.edu.jo (A.F.E.).

### ORCID

Khaleel I. Assaf: 0000-0003-4331-8492

Abdussalam K. Qaroush: 0000-0001-6549-7693

Bernhard Rieger: 0000-0002-0023-884X

Ala'a F. Eftaiha: 0000-0003-4285-2546

### Funding

This project was funded by the Deanship of Scientific Research at the Hashemite University (Grant number: 23/2018).

### Notes

The authors declare no competing financial interest.

## ■ ACKNOWLEDGMENTS

F.M.M. is grateful to the Scientific Research Fund (Ministry of Higher Education and Scientific Research, Jordan) for the financial support. K.I.A. acknowledges the Computational Laboratory for Analysis, Modeling, and Visualization (Jacobs University Bremen, Germany) for access to computation resources.

## ■ ABBREVIATIONS

DOP, dopamine; TYR, tyramine; PEA, phenylethylamine; EPN, epinephrine; MEA, monoethanolamine; RR'N-CO<sub>2</sub><sup>-</sup>Na<sup>+</sup>, sodium carbamate; RR'N-CO<sub>2</sub>H, carbamic acid; RR'N-CO<sub>2</sub><sup>-</sup>, carbamate carbonate; RO-CO<sub>2</sub><sup>-</sup>, organic carbonate; HSQC, heteronuclear single quantum coherence; DFT, density functional theory



## REFERENCES

- (1) Smit, B.; Reimer, J. A.; Oldenburg, C. M.; Bourg, I. C. *Introduction to Carbon Capture and Sequestration*; Berkeley Lectures on Energy; Imperial College Press, 2013; Vol. 1.
- (2) COP21 Paris Agreement, European Commission, [Http://Ec.Europa.Eu/Clima/Policies/International/Negotiations/Paris/Index\\_en.Htm](http://Ec.Europa.Eu/Clima/Policies/International/Negotiations/Paris/Index_en.Htm).
- (3) COP24 Katowice Conference, Poland, [Https://Cop24.Gov.Pl/](https://Cop24.Gov.Pl/).
- (4) Bui, M.; Adjiman, C. S.; Bardow, A.; Anthony, E. J.; Boston, A.; Brown, S.; Fennell, P. S.; Fuss, S.; Galindo, A.; Hackett, L. A.; et al. Carbon Capture and Storage (CCS): The Way Forward. *Energy Environ. Sci.* **2018**, *11*, 1062–1176.
- (5) Jonge, M. M. J. de; Daemen, J.; Loriaux, J. M.; Steinmann, Z. J. N.; Huijbregts, M. A. J. Life Cycle Carbon Efficiency of Direct Air Capture Systems with Strong Hydroxide Sorbents. *Int. J. Greenhouse Gas Control* **2019**, *80*, 25–31.
- (6) Aresta, M. *Carbon Dioxide as Chemical Feedstock*; John Wiley and Sons, 2010.
- (7) Kortunov, P. V.; Siskin, M.; Baugh, L. S.; Calabro, D. C. *In Situ* Nuclear Magnetic Resonance Mechanistic Studies of Carbon Dioxide Reactions with Liquid Amines in Aqueous Systems: New Insights on Carbon Capture Reaction Pathways. *Energy Fuels* **2015**, *29*, 5919–5939.
- (8) Heldebrant, D. J.; Yonker, C. R.; Jessop, P. G.; Phan, L. Organic Liquid CO<sub>2</sub> Capture Agents with High Gravimetric CO<sub>2</sub> Capacity. *Energy Environ. Sci.* **2008**, *1*, 487–493.
- (9) Roger, B. R. Process for Separating Acidic Gases. Process for Separating Acidic Gases by Roger Bottoms. US Patent US17839011930.
- (10) Sartori, G.; Savage, D. W. Sterically Hindered Amines for Carbon Dioxide Removal from Gases. *Ind. Eng. Chem. Fund.* **1983**, *22*, 239–249.
- (11) Bougie, F.; Iliuta, M. C. Sterically Hindered Amine-Based Absorbents for the Removal of CO<sub>2</sub> from Gas Streams. *J. Chem. Eng. Data* **2012**, *57*, 635–669.
- (12) Bates, E. D.; Mayton, R. D.; Ntai, I.; Davis, J. H. CO<sub>2</sub> Capture by a Task-Specific Ionic Liquid. *J. Am. Chem. Soc.* **2002**, *124*, 926–927.
- (13) Park, Y.; Lin, K.-Y. A.; Park, A.-H. A.; Petit, C. Recent Advances in Anhydrous Solvents for CO<sub>2</sub> Capture: Ionic Liquids, Switchable Solvents, and Nanoparticle Organic Hybrid Materials. *Front. Energy Res.* **2015**, *3*, 42.
- (14) Rajamanickam, R.; Kim, H.; Park, J.-W. Tuning Organic Carbon Dioxide Absorbents for Carbonation and Decarbonation. *Sci. Rep.* **2015**, *5*, 10688.
- (15) Heldebrant, D. J.; Koech, P. K.; Ang, M. T. C.; Liang, C.; Rainbolt, J. E.; Yonker, C. R.; Jessop, P. G. Reversible Zwitterionic Liquids, the Reaction of Alkanol Guanidines, Alkanol Amidines, and Diamines with CO<sub>2</sub>. *Green Chem.* **2010**, *12*, 713–721.
- (16) Kortunov, P. V.; Siskin, M.; Baugh, L. S.; Calabro, D. C. *In Situ* Nuclear Magnetic Resonance Mechanistic Studies of Carbon Dioxide Reactions with Liquid Amines in Non-Aqueous Systems: Evidence for the Formation of Carbamic Acids and Zwitterionic Species. *Energy Fuels* **2015**, *29*, 5940–5966.
- (17) Eftaiha, A. F.; Qaroush, A. K.; Assaf, K. I.; Alsoubani, F.; Markus Pehl, T.; Troll, C.; El-Barghouthi, M. I. Bis-Tris Propane in DMSO as a Wet Scrubbing Agent: Carbamic Acid as a Sequestered CO<sub>2</sub> Species. *New J. Chem.* **2017**, *41*, 11941–11947.
- (18) Qaroush, A. K.; Assaf, K. I.; Al-Khateeb, A.; Alsoubani, F.; Nabih, E.; Troll, C.; Rieger, B.; Eftaiha, A. F. Pentaerythritol-Based Molecular Sorbent for CO<sub>2</sub> Capturing: A Highly Efficient Wet Scrubbing Agent Showing Proton Shuttling Phenomenon. *Energy Fuels* **2017**, *31*, 8407–8414.
- (19) Anastas, P. T.; Warner, J. C. *Green Chemistry: Theory and Practice*; Oxford University Press, 2000.
- (20) Beach, E. S.; Cui, Z.; Anastas, P. T. Green Chemistry: A Design Framework for Sustainability. *Energy Environ. Sci.* **2009**, *2*, 1038–1049.
- (21) Anastas, P.; Eghbali, N. Green Chemistry: Principles and Practice. *Chem. Soc. Rev.* **2010**, *39*, 301–312.
- (22) Erythropel, H. C.; Zimmerman, J. B.; de Winter, T. M.; Pettitjean, L.; Melnikov, F.; Lam, C. H.; Lounsbury, A. W.; Mellor, K. E.; Janković, N. Z.; Tu, Q.; et al. The Green ChemistREE: 20 Years after Taking Root with the 12 Principles. *Green Chem.* **2018**, *20*, 1929–1961.
- (23) Qaroush, A. K.; Castillo-Molina, D. A.; Troll, C.; Abu-Daabes, M. A.; Alsayouri, H. M.; Abu-Surrah, A. S.; Rieger, B. [N]-Oligourea-Based Green Sorbents with Enhanced CO<sub>2</sub> Sorption Capacity. *ChemSusChem* **2015**, *8*, 1618–1626.
- (24) Yang, Y.; Song, L.; Peng, C.; Liu, E.; Xie, H. Activating Cellulose via Its Reversible Reaction with CO<sub>2</sub> in the Presence of 1,8-Diazabicyclo[5.4.0]Undec-7-Ene for the Efficient Synthesis of Cellulose Acetate. *Green Chem.* **2015**, *17*, 2758–2763.
- (25) Gunnarsson, M.; Theliander, H.; Hasani, M. Chemisorption of Air CO<sub>2</sub> on Cellulose: An Overlooked Feature of the Cellulose/NaOH(Aq) Dissolution System. *Cellulose* **2017**, *24*, 2427–2436.
- (26) Gunnarsson, M.; Bernin, D.; Östlund, Å.; Hasani, M. The CO<sub>2</sub> Capturing Ability of Cellulose Dissolved in NaOH(aq) at Low Temperature. *Green Chem.* **2018**, *20*, 3279–3286.
- (27) Xie, H.; Zhang, S.; Li, S. Chitin and Chitosan Dissolved in Ionic Liquids as Reversible Sorbents of CO<sub>2</sub>. *Green Chem.* **2006**, *8*, 630–633.
- (28) Sun, X.; Huang, C.; Xue, Z.; Mu, T. An Environmentally Benign Cycle To Regenerate Chitosan and Capture Carbon Dioxide by Ionic Liquids. *Energy Fuels* **2015**, *29*, 1923–1930.
- (29) Eftaiha, A. F.; Alsoubani, F.; Assaf, K. I.; Nau, W. M.; Troll, C.; Qaroush, A. K. Chitin-Acetate/DMSO as a Supramolecular Green CO<sub>2</sub>-Phile. *RSC Adv.* **2016**, *6*, 22090–22093.
- (30) Eftaiha, A. F.; Alsoubani, F.; Assaf, K. I.; Troll, C.; Rieger, B.; Khaled, A. H.; Qaroush, A. K. An Investigation of Carbon Dioxide Capture by Chitin Acetate/DMSO Binary System. *Carbohydr. Polym.* **2016**, *152*, 163–169.
- (31) Qaroush, A. K.; Assaf, K. I.; Bardaweel, S. K.; Al-Khateeb, A.; Alsoubani, F.; Al-Ramahi, E.; Masri, M.; Brück, T.; Troll, C.; Rieger, B.; et al. Chemisorption of CO<sub>2</sub> by Chitosan Oligosaccharide/DMSO: Organic Carbamate–Carbonate Bond Formation. *Green Chem.* **2017**, *19*, 4305–4314.
- (32) Carrera, G. V. S. M.; Jordao, N.; Branco, L. C.; Nunes da Ponte, M. CO<sub>2</sub> Capture Systems Based on Saccharides and Organic Superbases. *Faraday Discuss.* **2015**, *183*, 429–444.
- (33) Eftaiha, A. F.; Qaroush, A. K.; Alsoubani, F.; Pehl, T. M.; Troll, C.; Rieger, B.; Al-Maythaly, B. A.; Assaf, K. I. A Green Sorbent for CO<sub>2</sub> Capture:  $\alpha$ -Cyclodextrin-Based Carbonate in DMSO Solution. *RSC Adv.* **2018**, *8*, 37757–37764.
- (34) Smaldone, R. A.; Forgan, R. S.; Furukawa, H.; Gassensmith, J. J.; Slawin, A. M. Z.; Yaghi, O. M.; Stoddart, J. F. Metal–Organic Frameworks from Edible Natural Products. *Angew. Chem., Int. Ed.* **2010**, *49*, 8630–8634.
- (35) Gassensmith, J. J.; Furukawa, H.; Smaldone, R. A.; Forgan, R. S.; Botros, Y. Y.; Yaghi, O. M.; Stoddart, J. F. Strong and Reversible Binding of Carbon Dioxide in a Green Metal–Organic Framework. *J. Am. Chem. Soc.* **2011**, *133*, 15312–15315.
- (36) Gassensmith, J. J.; Kim, J. Y.; Holcroft, J. M.; Farha, O. K.; Stoddart, J. F.; Hupp, J. T.; Jeong, N. C. A Metal–Organic Framework-Based Material for Electrochemical Sensing of Carbon Dioxide. *J. Am. Chem. Soc.* **2014**, *136*, 8277–8282.
- (37) Hartlieb, K. J.; Peters, A. W.; Wang, T. C.; Deria, P.; Farha, O. K.; Hupp, J. T.; Stoddart, J. F. Functionalised Cyclodextrin-Based Metal–Organic Frameworks. *Chem. Commun.* **2017**, *53*, 7561–7564.
- (38) Qaroush, A. K.; Alshamaly, H. S.; Alazzez, S. S.; Abeskhron, R. H.; Assaf, K. I.; Eftaiha, A. F. Inedible Saccharides: A Platform for CO<sub>2</sub> Capturing. *Chem. Sci.* **2018**, *9*, 1088–1100.
- (39) Bhattacharyya, S.; Shah, F. U. Ether Functionalized Choline Tethered Amino Acid Ionic Liquids for Enhanced CO<sub>2</sub> Capture. *ACS Sustainable Chem. Eng.* **2016**, *4*, 5441–5449.
- (40) Li, X.; Hou, M.; Zhang, Z.; Han, B.; Yang, G.; Wang, X.; Zou, L. Absorption of CO<sub>2</sub> by Ionic Liquid/Polyethylene Glycol Mixture

and the Thermodynamic Parameters. *Green Chem.* **2008**, *10*, 879–884.

(41) Latini, G.; Signorile, M.; Crocellà, V.; Bocchini, S.; Pirri, C. F.; Bordiga, S. Unraveling the CO<sub>2</sub> Reaction Mechanism in Bio-Based Amino-Acid Ionic Liquids by Operando ATR-IR Spectroscopy *Catal. Today* **2019**, DOI: 10.1016/j.cattod.2018.12.050, in press.

(42) Yuan, S.; Chen, Y.; Ji, X.; Yang, Z.; Lu, X. Experimental Study of CO<sub>2</sub> Absorption in Aqueous Cholinium-Based Ionic Liquids. *Fluid Phase Equilib.* **2017**, *445*, 14–24.

(43) Saptal, V. B.; Bhanage, B. M. Bifunctional Ionic Liquids Derived from Biorenewable Sources as Sustainable Catalysts for Fixation of Carbon Dioxide. *ChemSusChem* **2017**, *10*, 1145–1151.

(44) Eftaiha, A. F.; Mustafa, F. M.; Alsoubani, F.; Assaf, K. I.; Qaroush, A. K. A Catecholamine Neurotransmitter: Epinephrine as a CO<sub>2</sub> Wet Scrubbing Agent. *Chem. Commun.* **2019**, *55*, 3449–3452.

(45) Solomons, T. W. G.; Fryhle, C. B.; Snyder, S. A. *Organic Chemistry*, 12<sup>th</sup> ed.; Wiley, 2016.

(46) Solubility of L-DOPA, <https://Www.Scbt.Com/Scbt/Product/Levodopa-59-92-7>.

(47) Til, H. P.; Falke, H. E.; Prinsen, M. K.; Willems, M. I. Acute and Subacute Toxicity of Tyramine, Spermidine, Spermine, Putrescine and Cadaverine in Rats. *Food Chem. Toxicol.* **1997**, *35*, 337–348.

(48) Potkin, S.; Karoum, F.; Chuang, L.; Cannon-Spoor, H.; Phillips, I.; Wyatt, R. Phenylethylamine in Paranoid Chronic Schizophrenia. *Science* **1979**, *206*, 470–471.

(49) <sup>15</sup>N Chemical Shift, <https://Wissen.Science-and-Fun.de/Chemistry/Spectroscopy/15N-Chemical-Shifts/>.